

# Strongly enhanced superconductivity in coupled $t$ - $J$ segments

Sahinur Reja<sup>1</sup>, Jeroen van den Brink<sup>1</sup> and Satoshi Nishimoto<sup>1,2</sup>

<sup>1</sup>*Institute for Theoretical Solid State Physics, IFW Dresden, 01171 Dresden, Germany*

<sup>2</sup>*Institute for Theoretical Physics, TU Dresden, 01069 Dresden, Germany*

(Dated: March 3, 2024)

The  $t$ - $J$  Hamiltonian is one of the cornerstones in the theoretical study of strongly correlated copper-oxide based materials. Using the density matrix renormalization group method we calculate the phase diagram of the one-dimensional  $t$ - $J$  chain in the presence of a periodic hopping modulation, as a prototype of coupled-segment models. While in the uniform 1D  $t$ - $J$  model near half-filling superconducting (SC) state dominates only at unphysically large values of the exchange coupling constant  $J/t > 3$ , we show that a small hopping and exchange modulation very strongly reduces the critical coupling to be as low as  $J/t \sim 1/3$  – well within the physical regime. The phase diagram as a function of the electron filling also exhibits metallic, insulating line phases and regions of phase separation. We suggest that a SC state is easily stabilized if  $t$ - $J$  segments creating local spin-singlet pairing are coupled to each other – another example is ladder system.

PACS numbers: 74.20.-z, 71.10.Fd, 71.45.Lr, 74.25.Dw

*Introduction* — Since its introduction at the end of the 1980's, the  $t$ - $J$  model Hamiltonian[1] has formed one of the cornerstones in the theoretical study of high temperature superconductors (HTSs). It is a minimal low-energy model for the electronic and magnetic structure of the copper-oxide planes in HTSs and can be derived from the Hubbard model in the strong coupling limit using second order perturbation theory[2]. Although the initial interest in the  $t$ - $J$  model focussed on its two-dimensional (2D) realization, its one-dimensional (1D) version, which is of direct relevance to for instance doped spin-chain materials, provides a number of interesting phases that are also observed in the 2D context, such as a spin gap phase and the occurrence of phase separation[3, 4]. The 1D  $t$ - $J$  model actually also displays a superconducting instability, even if all this is in a parameter range where the ratio of the exchange constant  $J$  and hopping  $t$ , near half-filling is  $J/t \sim 3$ , which is not of relevance to real materials – the HTSs are rather in the regime where  $J/t \sim 1/3$ . In the latter regime quasi-1D systems e.g.,  $t$ - $J$  ladders can support superconductivity [6–9] which is related to the substantial binding energy for two holes in even-leg ladders, giving rise to the presence of preformed Cooper pairs on the rungs. However, in a 1D system this binding energy vanishes for physically relevant values of  $J/t$  [10].

In this Letter we consider the 1D  $t$ - $J$  Hamiltonian in the presence of a periodic local modulation of  $t$  and  $J$ : within segments of length  $S_l$  the hopping and exchange are constant, but the coupling *between* these segments is somewhat weaker, see Fig. 1. In a solid such a local modulation might for instance result from a periodic structural modification or from electronic self-organization. Using the density matrix renormalization group (DMRG) method we establish that for hole-doped systems close to half filling in the presence of a weak modulation not only a spin-gap forms but also that the holes pair-up already for moderate values of  $J/t$ . A calculation of the Luttinger parameter shows the formation of a superconducting (SC) state in a large region of the phase dia-

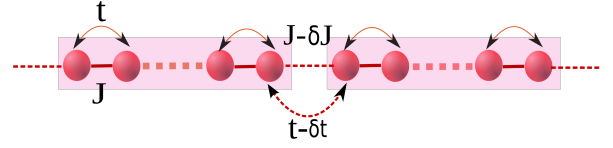


FIG. 1: (Color online) Schematic of the model for coupled  $t$ - $J$  segments. Here  $t$  and  $J$  are the hopping integral and exchange interaction respectively with corresponding reduction  $\delta t$  and  $\delta J$  only for the bonds connecting end sites of the segments.

gram, also in the physically relevant low-doping regime with  $J/t \sim 1/3$ . The transition point weakly depends on segment length and apart from superconductivity also metallic, insulating and phase separated regions are present in the calculated phase diagram.

*Model and Method* — To investigate the effect of coupling of segments forming a 1D chain, we consider the model Hamiltonian  $H = H_0 + H_\delta$  where  $H_0$  is the uniform 1D  $t$ - $J$  Hamiltonian  $H_0 = -t \sum_{i\sigma} (c_{i,\sigma}^\dagger c_{i+1,\sigma} + H.c.) + J \sum_i (\mathbf{S}_i \cdot \mathbf{S}_{i+1} - \frac{1}{4} n_i n_{i+1})$ , where the sum is over all integers  $i$  labeling the sites that make up the chain and  $H_\delta$  describes the local modulation and

$$H_\delta = \delta t \sum_{j\sigma} (c_{j.S_l,\sigma}^\dagger c_{j.S_l+1,\sigma} + H.c.) - \delta J \sum_j (\mathbf{S}_{j.S_l} \cdot \mathbf{S}_{j.S_l+1} - \frac{n_{j.S_l} n_{j.S_l+1}}{4}), \quad (1)$$

where the sum is over all integers  $j$ .  $H_\delta$  represents the reduction in hopping  $\delta t$  and exchange interaction  $\delta J$  on the bonds connecting end sites of segments of length  $S_l$ . The modulated bond consist of the rightmost site of  $j^{th}$  segment and next site to it, which are indexed by  $j.S_l$  and  $(j.S_l + 1)$  respectively – a schematic of the model is shown in Fig. 1. In the Hamiltonian  $c_{i\sigma}^\dagger$  is the electron creation operator at site  $i$  with spin  $\sigma$ ,  $\mathbf{S}_i$  is the spin- $\frac{1}{2}$  operator, and  $n_i$  the electronic number operator. In order to stay within the perturbative framework in which the

$t$ - $J$  model is derived from the Hubbard Hamiltonian, we retain the direct relation between  $\delta t$  and  $\delta J$  from second order perturbation theory: as  $J = 4t^2/U$ , where  $U$  is the onsite Coulomb repulsion, we have that

$$\frac{J - \delta J}{J} = \left( \frac{t - \delta t}{t} \right)^2 \quad (2)$$

In units of  $t$ , we are thus left with only two energy scales:  $\delta t/t$  and  $J/t$ . The parameter  $\delta J/J$  is fixed by the relation in Eq. [2]. Clearly for  $\delta t = 0$  the model reduces to the regular 1D  $t$ - $J$  Hamiltonian. The electron density is denoted by  $n$ .

The quantities of interest e.g., Luttinger parameter, spin gap, binding energy are calculated by DMRG method[11, 12] on a lattice with upto 288 sites and finite size extrapolations are performed to obtain them in thermodynamic limit (see supplemental material). As we have studied the system with segment length  $S_l = 2, 4, 6, 8, 12$  we choose the system size  $L = 48, 96, 144, 192, 240, 288$ . This allows us to have the number of electrons  $N = nL$  and the number of segments in the system to be even so that the ground state corresponds to total spin  $S_z^T = 0$ . All the results are obtained with upto 2000 basis states, 15 sweeps and typical discarded weight  $\sim 10^{-8}$  leading to error in energy of the same order.

*Spin gap and pair binding* — We start our discussion with the calculations for the spin gap  $\Delta_s$  in the system with coupled segments. The usual  $t$ - $J$  model (i.e.,  $\delta t = 0$ ) in 1D has a spin gap phase, as is found in the studies by exact diagonalization in small systems[3], variational methods[22], RG analysis[23] and more recently by DMRG method[4]. But in all the studies spin gap phase appears only at low *electron* density and at large exchange  $J/t > 2$ , a parameter regime that is barely relevant to real materials. We show below that the spin gap phase can appear at small  $J/t$  and for weak hole doping (i.e.,  $n \rightarrow 1$ ) when a non-zero  $\delta t$  is introduced.

The singlet-triplet excitation energy is given by the energy difference  $\Delta_s = E(N, S_z^T = 1) - E(N, S_z^T = 0)$ . Here  $E(N, S_z^T)$  is the ground state energy with quantum numbers  $N$  and total  $z$ -component of spins  $S_z^T$ . At half-filling,  $n = 1$ , the uniform  $t$ - $J$  model corresponds to a Mott insulator with zero spin gap. But if  $\delta t$  is switched on, a spin gap  $\Delta_s$  forms and increases monotonically, see Fig. 2(a). The gap reaches its maximum in the limit  $\delta t/t = 1$ , where it corresponds to the finite size gap of decoupled Heisenberg segments. However, the situation changes drastically when holes are doped into the system, see Fig. 2(b) and (c). The overall spin-gap is much reduced but kept to be finite, and reaches its maximum for *small*  $\delta t/t$  and gradually vanishes for larger values of the hopping modulation. Fig. 2(b) shows the spin gap  $\Delta_s$  for  $J/t = 0.8$  at different  $\delta t$  in the limiting density  $n \rightarrow 1$  which corresponds to putting only two holes in different system sizes and extrapolating  $\Delta_s$  to thermodynamic limit (see supplemental material). The calcu-

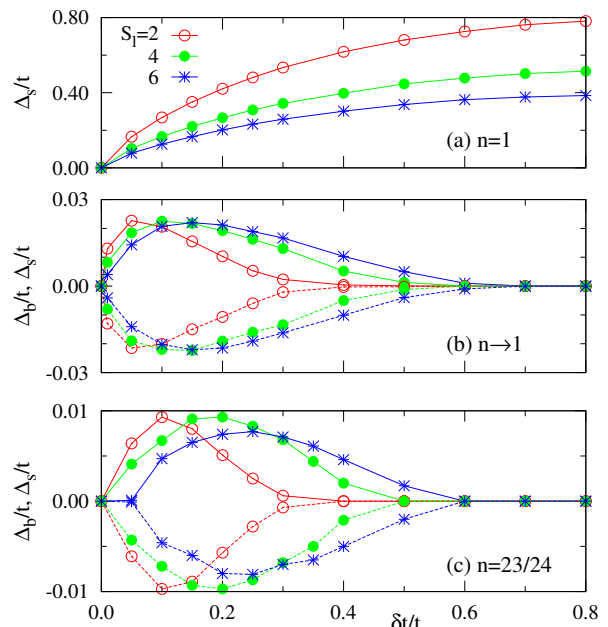


FIG. 2: (Color online) The spin gap  $\Delta_s$  and binding energy  $\Delta_b$  at  $J/t = 0.8$  as a function of  $\delta t$  for (a) half filling  $n = 1$ , (b) in the limit of half filling  $n \rightarrow 1$  i.e., 2 holes in the system and (c)  $n = 23/24$ . The empty circles (red), filled circles (green) and starred points (blue) connected with solid lines represent the spin gap for segment size  $S_l = 2, 4$  and  $6$  respectively. The corresponding circles and points connected with dotted lines represent binding energy.

lations were done for segment sizes  $S_l = 2, 4$  and  $6$ . Surprisingly, a very small  $\delta t = 0.01$  is already enough to produce a sizable spin gap in the system. The spin gap increases first as in half-filled case, but then decreases to zero for larger  $\delta t$ . It is interesting that the maximum of the spin gap is not really sensitive to the segment size. We notice that the occurrence of maximum of  $\Delta_s$  shifts to higher  $\delta t$  if we increase segment size  $S_l$ . It is related to slower reduction of (electron or hole) bandwidth by  $\delta t$  for larger  $S_l$ . Also shown in the figures is the pair binding energy, which measures the stability of pairing and is defined as  $\Delta_b = E(N \pm 2, S_z^T = 0) + E(N, S_z^T = 0) - 2E(N \pm 1, S_z^T = \pm 1/2)$ . The plot for  $\Delta_b$  is shown in Fig. 2(b) for  $S_l = 2, 4$  and  $6$  with the same points and colors as  $\Delta_s$  but connected by dotted lines. The negative values of  $\Delta_b$  indicates the stability of pairing and a relation  $\Delta_s = |\Delta_b|$  in a metallic (M) regime suggests an occurrence of spin-singlet SC state. The spin gap and pair binding energy at a finite hole density of  $n = 23/24$  are shown in Fig. 2(c). Compared to the limit of half filling  $n \rightarrow 1$ , their magnitudes are smaller but the overall behaviors are almost unchanged.

*Superconductivity and Phase diagram*— The DMRG calculations allow us to map out the phase diagram for the modulated 1D  $t$ - $J$  Hamiltonian including also potential states. It should be noted that the uniform  $t$ - $J$  model shows a transition from M to SC state at  $J/t \geq 2$  in low

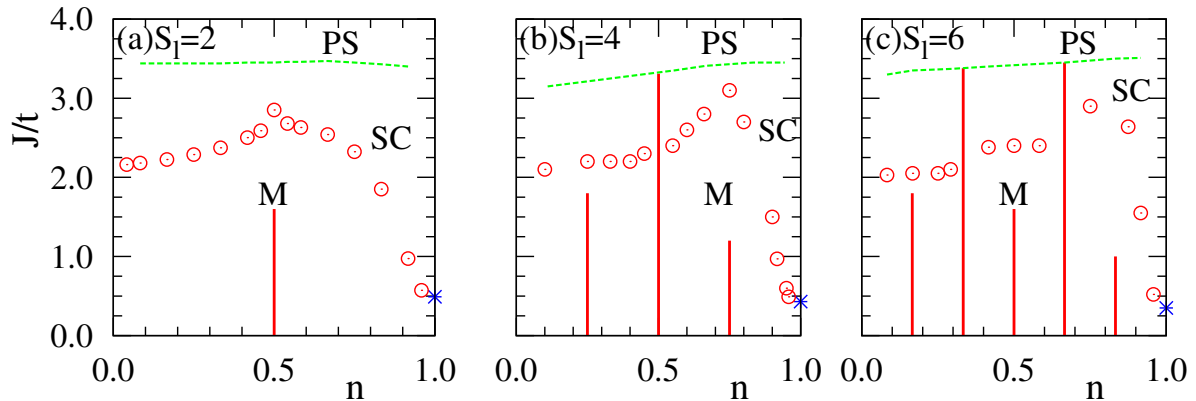


FIG. 3: (Color online) (a)-(c) Phase diagrams on  $n$ - $J/t$  plane at  $\delta t/t = 0.2$  for  $S_l = 2, 4$  and  $6$  systems respectively containing different phases: Superconducting (SC), Metallic (M) and Phase separated (PS) as indicated. The points (empty circles) represent M to SC transition and the point (star) indicates density  $n \rightarrow 1$  (system with 2 holes). The vertical lines at different commensurate fillings represent insulating line-phases.

electron density regime. An even higher  $J/t$  is necessary to get SC phase with increasing electron density[4]. In order to examine the possibility of superconductivity in system with coupled segments at different electronic density  $n$ , we determine the metal-SC transition by calculating the Luttinger parameter:  $K_\rho < 1$  for a paramagnetic metal and  $K_\rho > 1$  for a superconductor. In the thermodynamic limit the Luttinger parameter is determined from the slope of the structure factor for the density-density correlation at wave vector  $k \rightarrow 0$  limit[13, 14]. To avoid difficulties in the calculation of real-space density-density correlations at large distances and the subsequent Fourier transform at small  $k$ , we calculate structure factor directly in momentum space[15] and extract  $K_\rho$  in thermodynamic limit by finite size scaling (see supplemental material). This requires calculating  $K_\rho$  for different system sizes (upto 288 sites).

We determined the crossing point  $K_\rho = 1$  for fixed different densities  $n$ , segment lengths  $S_l$ , and modulation strengths  $\delta t$ , that separates the M and SC phases as a function of  $J/t$ . The critical value is denoted by  $J^c/t$  hereafter. At very large  $J$ , the system separates into electron- and hole-rich region and the onset of phase separation (PS) has been determined by inverse compressibility (see supplemental material). The resulting  $n$ - $J/t$  phase diagrams containing PS, M and SC phases are shown in Fig. 3(a)-(c) for  $\delta t/t = 0.2$  and  $S_l = 2, 4$  and  $6$ , respectively. The (blue) star symbol represents the critical point  $J^c/t$  in  $n \rightarrow 1$  limit. It is remarkable that close to half filling (even for a system with only two holes i.e.,  $n \rightarrow 1$ )  $J^c/t$  is significantly reduced for all the cases of three  $S_l$ 's as shown in Fig. 3. Apparently, the critical value can be as small as  $J^c/t \sim 0.35$  for a relatively weak modulation  $\delta t/t = 0.2$ .

This observation motivates to study how the critical point  $J^c/t$  changes as a function of  $\delta t/t$ . Since a large reduction of  $J^c/t$  can be acquired near half filling, we fix

the filling at  $n = 23/24$  and estimate the critical point. The critical value  $J^c/t$  at  $n = 23/24$  is shown in Fig. 4 for  $S_l = 2, 4, 6, 8, 12$ . For each segment length even a weak modulation  $\delta t$  causes a large drop in  $J^c/t$  from  $\sim 3.2$  at the uniform case  $\delta t = 0$ . Depending on the segment size the lowest  $J_c/t$  is reached for  $\delta t/t$  between  $\sim 0.1$  and  $\sim 0.3$ . The calculations imply that an increase of  $\delta t$  helps electrons in each segment to form pairs which can move easily unless  $\delta t/t$  becomes too large, which then tends to localize electrons on individual segments for large  $\delta t/t$ . This explains the steep minimum and then slow rise in  $J^c/t$ . At small  $\delta t/t$ , the transition point  $J^c/t$  increases with  $S_l$  because the pair formation gets weakened as the number of sites in a segment becomes larger. Ultimately, at very large  $S_l$ , this situation will correspond to the uniform  $t$ - $J$  model. On the other hand at large  $\delta t/t$ , the pair formation is most effective but the movement of pairs is restricted due to the narrowing of bandwidth and a high  $J^c/t$  is given accordingly. An intriguing thing is that for  $S_l = 12$  the strong reduction of  $J^c/t$  is obtained despite  $J^c/t \sim 3.2$  for any  $\delta t/t$  in the  $S_l \rightarrow \infty$  limit. It means that a system with  $S_l = 12$  is still far from the uniform  $t$ - $J$  model. We also notice a sharp decrease in  $J^c/t$  as we increase  $S_l = 2$  to  $12$  initially at large  $\delta t/t$  and then almost saturates. To explain this behavior, we calculate the spin gap of decoupled segments (i.e.,  $\delta t/t = 1$ ) of different sizes starting from  $S_l = 2$ . As expected, we see a sharp decrease of spin gap with  $S_l$  as shown in the inset of Fig. 4. Plots in Fig. 4 also explains the appearance of finite spin gap discussed in Fig. 2(c) for density  $n = 23/24$  at  $J/t = 0.8$ . The critical  $J^c/t$  where the M to SC transition occurs is lower than  $J/t = 0.8$  for some range of  $\delta t/t$  and for different  $S_l$ . This means the system develops a finite spin gap entering into SC phase.

*Insulating line phases* — Unlike the uniform  $t$ - $J$  model, we notice some insulating regions (vertical lines in Fig. 3) appearing at various commensurate fillings. This type of

insulating region at particular commensurate fillings has been discussed in ladder systems[20]. Due to the restriction in hopping as we introduce  $\delta t$ , the electrons may form super structure in each segment which leads to insulating behavior of the system. The insulating to M transition at  $n = 1/2$  which is shown in Fig. 3(a) for  $S_l = 2$  system has been discussed in terms of melting of Mott insulating states[21]. We briefly recap its intuitive understanding which will guide us to understand the insulating regions at other fillings and  $S_l = 4, 6$  systems.

Let us first consider  $S_l = 2$  system with no exchange interaction i.e.,  $J \rightarrow 0$  in  $U \rightarrow \infty$  limit. Then the tight binding model with  $\delta t > 0$  at  $n = 1/2$  forms bonding and antibonding states with spin  $\sigma$  i.e.,  $t$ -dimer states:  $|t-dim\rangle_\sigma = (|\sigma\ 0\rangle \pm |0\ \sigma\rangle)/\sqrt{2}$  separated by a gap  $\Delta_d = 2\delta t$  at each segment. Due to this  $t$ -dimerization one electron per segment is in the bonding state at this commensurate density of  $n = 1/2$  and the system becomes a Mott insulator. But if we increase  $J$ , a tendency to make singlet pairs is introduced at each segment due to  $J$ -dimerization which leads to a transition to M states. If we increase  $J$  further where  $J$ -dimerization dominates, the system with these singlet pairs becomes SC and finally goes to PS at large  $J$ . Such a melting of insulating states happen also in  $S_l = 4$  system at  $n = 1/4, 3/4$  and  $S_l = 6$  system at  $n = 1/6, 3/6, 5/6$  as shown in Fig. 3(b) and (c), respectively. No effective pairing with odd number of electrons in a segment at these electronic fillings causes the melting of insulating states with increasing  $J$ . However, even number of electrons in a segment as in  $S_l = 4$  system at  $n = 1/2$  and  $S_l = 6$  system at  $n = 2/6, 4/6$  prevent such melting of insulating states by making effective pairing between themselves even with increasing  $J$ . So the insulating states continue to exist until the PS boundary at these fillings with increasing  $J$  as shown in Fig. 3(b) and (c). These insulating line phases and metal-insulator transitions are captured by calculating charge gap defined as  $\Delta_c = (E(N+2) + E(N-2) - 2E(N))/2$  for different values of  $J$ .

*Conclusions:* We have shown using density matrix renormalization group method that a metal to superconducting transition can occur in a physically relevant regime of exchange interaction and hopping (i.e.,  $J/t \sim 1/3$ ) in 1D system with coupled  $t$ - $J$  segments. A moderate modulation  $\delta t/t$  in the hopping causes a superconducting state for electron densities close to half filling. As compared to uniform 1D  $t$ - $J$  model, this implies an order of magnitude reduction in critical exchange interaction to hopping ratio. We have presented full  $n$ - $J$  phase diagrams at  $\delta t/t = 0.2$  with different segment sizes containing besides

phase separation, metallic and superconducting phases also insulating line phases at commensurate doping concentrations. These results may be of relevance to certain quasi 1D materials, including cuprates in which typical exchange coupling is  $J \sim t/3$ [16]. An example is the spin-Peierls system  $\text{CuGeO}_3$ [17] which consists of linear spin- $\frac{1}{2}$   $\text{CuO}_2$  chains with alternating exchange coupling

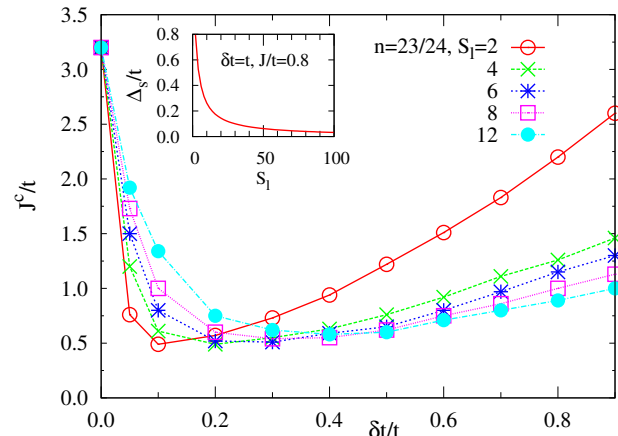


FIG. 4: (Color online) This shows the transition from metallic to superconducting phase at density  $n = 23/24$  as a function  $t_2$  and for systems with segment sizes 2, 4, 6, 8, 12 as indicated. In the inset we plot  $\Delta_s$  for systems with decoupled segments of different sizes at  $J/t = 0.8$ .

and hopping strength, corresponding to a  $S_l = 2$  system in our language. The results above suggest that doping with few holes may turn the system to be superconducting. Such values of exchange coupling and hopping strengths can in principle also be achieved in 1D ultracold fermionic quantum gases[18] and with polar molecules[19] on optical lattices. It will be most interesting to establish whether in such quantum simulator experiments a superconducting state can be stabilized by a relatively benign modulation of the 1D  $t$ - $J$  Hamiltonian as we propose here. In this Letter, the segments are open chain coupled linearly as a simplest 1D case. However, any shape of segment can be allowed if it creates locally finite spin excitation gap. The network between the segments would be also flexible. We think that this simple condition possibly makes a great help for superconducting material design. For example, the ladder  $t$ - $J$  system is a special case of the coupled-segment systems.

*Acknowledgments:* This work is supported by SFB 1143 of the Deutsche Forschungsgemeinschaft.

- 
- [1] F. C. Zhang and T. M. Rice, Phys. Rev. B **37**, 3759 (1988).  
 [2] K. A. Chao, J. Spalek, and A. M. Oles, J. Phys. C **10**, L271 (1977)

- [3] Masao Ogata, M. U. Luchini, S. Sorella, and F. F. Assaad, Phys. Rev. Lett. **66**, 2388 (1991)  
 [4] Alexander Moreno et al., Phys. Rev. B **83**, 205113 (2011)  
 [5] Chen Cheng et al., EPL **110**110, 37002 (2015)

- [6] Masatomo Uehara et al., J. Phys. Soc. Jpn. **65**, 2764-2767 (1996)
- [7] Ikuo Ichinose and Tetsuo Matsui, Phys. Rev. B **57**, 13790 (1998)
- [8] E. Dagotto, J. Riera, and D.J. Scalapino, Phys. Rev. B **45**, 5744 (1992)
- [9] Steven R. White and D. J. Scalapino, Phys. Rev. B **55**, 6504 (1997)
- [10] Zheng Zhu et al., Scientific Reports **4**, 5419 (2014)
- [11] S. R. White, Phys. Rev. Lett. **69**, 2863 (1992)
- [12] U. Schollwock, Rev. Mod. Phys. **77**, 259 (2005)
- [13] T. Giamarchi, Quantum Physics in One Dimension (Clarendon, Oxford, UK, 2004)
- [14] R. T. Clay et al., Phys. Rev. B **59**, 4665 (1999)
- [15] S. Ejima et al., Eurphys. Lett. **70**, 492 (2005)
- [16] M. S. Hybertsen et al., Phys. Rev. B **41**, 11068 (1990)
- [17] Masashi Hase et al., Phys. Rev. Lett. **70**, 3651 (1993)
- [18] Andre Eckardt and Maciej Lewenstein, Phys. Rev. A **82**, 011606(R) (2010)
- [19] A. V. Gorshkov et al., Phys. Rev. Lett. **107**, 11531 (2011)
- [20] Steven R. White et al., Phys. Rev. B **65**, 165122 (2002)
- [21] S. Nishimoto and Y. Ohta., Phys. Rev. B **59**, 4738 (1999)
- [22] Y. C. Chen and T. K. Lee, Phys. Rev. B **47**, 11548 (1993)
- [23] M. Nakamura et al., Phys. Rev. Lett. **79**, 3214 (1997)

# Supplementary Material for “Strongly enhanced superconductivity in coupled $t$ - $J$ segments”

Sahinur Reja<sup>1</sup>, Jeroen van den Brink<sup>1</sup> and Satoshi Nishimoto<sup>1,2</sup>

<sup>1</sup>*Institute for Theoretical Solid State Physics, IFW Dresden, 01171 Dresden, Germany*

<sup>2</sup>*Institute for Theoretical Physics, TU Dresden, 01069 Dresden, Germany*

(Dated: March 3, 2024)

Here we present a detailed plots of finite size scaling analysis to get spin gap, charge gap and Luttinger parameter in thermodynamic limit. Luttinger parameter has been used to determine the transition between metallic to superconducting phases whereas spin gap and binding energy indicate the stability of pairing of electrons. Insulating line phases are captured by finite charge gap and onset of phase separation is obtained from inverse compressibility.

We use DMRG method[1, 2] to study the system consisting of coupled  $t$ - $J$  segments in presence of periodic hopping modulations on a lattice with total upto 288 sites and different segment size  $S_l$ . We calculate each of the quantities of interest e.g., Luttinger parameter, spin gap, binding energy, charge gap in thermodynamic limit by finite size extrapolation. As we have studied the system with segment length  $S_l = 2, 4, 6, 8, 12$  we choose the system size  $L = 48, 96, 144, 192, 240, 288$  and more in some calculations. This allows us to have the number of electrons  $N = nL$  and the number of segments in the system to be even so that the ground state corresponds to total spin  $S_z^T = 0$ . All the results are obtained with at least 500 basis states, 15 sweeps and typical discarded weight  $\sim 10^{-8}$  leading to error in energy of the same order.

We make use of Luttinger parameter  $K_\rho$  to find the metallic ( $K_\rho < 1$ ) to superconducting ( $K_\rho > 1$ ) transition as a function of exchange coupling  $J$  and electronic density  $n$ . This enables us to map out the  $n - J$  phase diagrams presented for  $S_l = 2, 4, 6$  systems. The spin gap and binding energy indicate the stability of electron pairing in superconducting state. Insulating line phases at different commensurate fillings are captured by charge gap calculation. Finally inverse compressibility has been used to estimate the phase separation boundary.

## SPIN GAP AND PAIR BINDING

Spin gap represents singlet to triplet excitation energy and is defined as:

$$\Delta_s = E(N, S_z^T = 1) - E(N, S_z^T = 0) \quad (1)$$

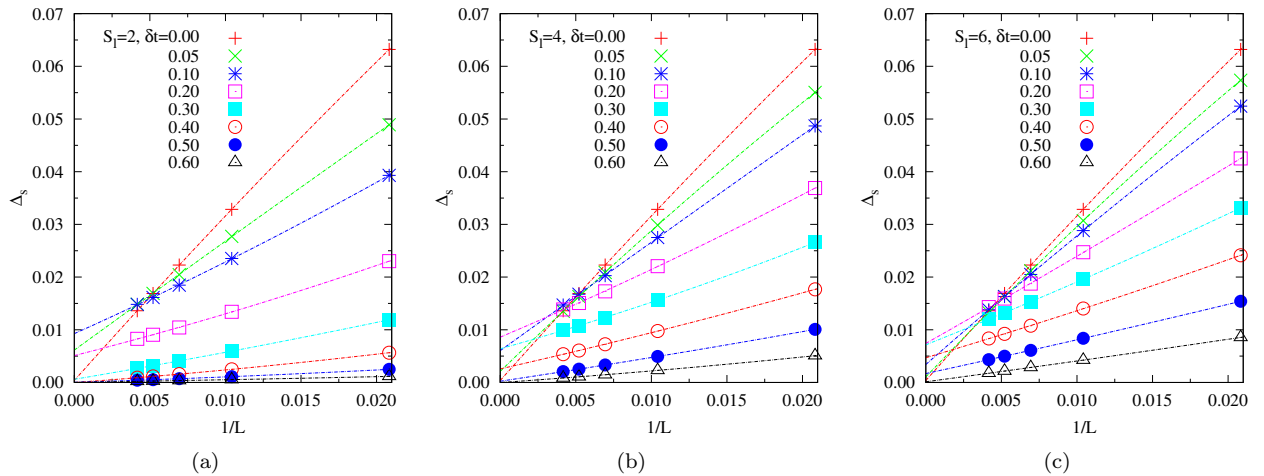


FIG. 1: (Color online) Spin gap extrapolation to thermodynamic limit at finite electronic filling  $n = 23/24$ . These plots are for different hopping modulation  $\delta t$  and segment size  $S_l = 2, 4, 6$  in (a), (b) and (c) respectively with exchange coupling  $J/t = 0.8$

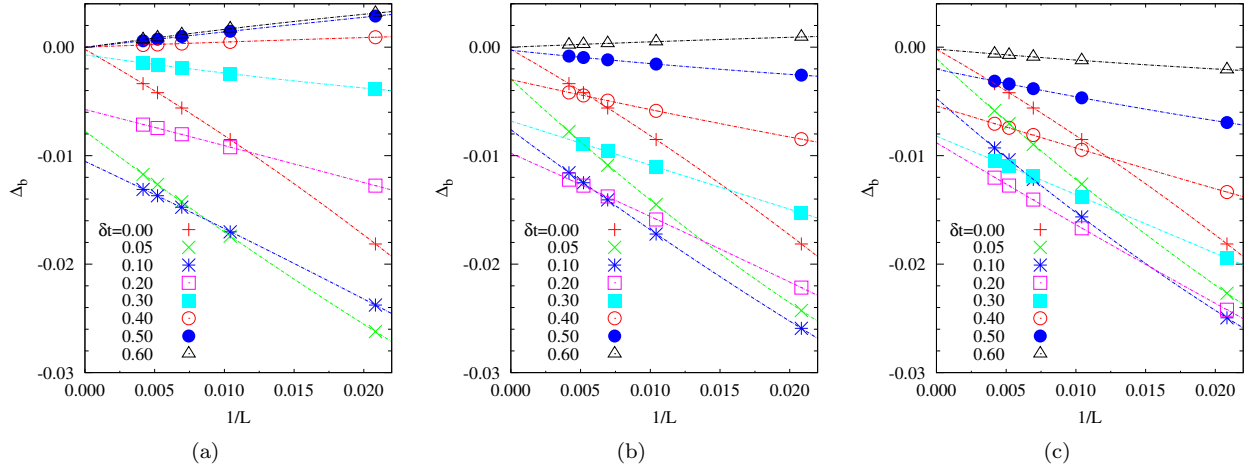


FIG. 2: (Color online) Binding energy extrapolation to thermodynamic limit at finite electronic filling  $n = 23/24$ . These plots are for different hopping modulation  $\delta t$  and segment size  $S_l = 2, 4, 6$  in (a), (b) and (c) respectively with exchange coupling is  $J/t = 0.8$

where  $E(N, S_z^T)$  is the ground state energy with quantum numbers  $N = nL$  and total  $z$ -component of spins  $S_z^T$ . Fig. 1 shows the finite size scaling of spin gap. We choose finite electronic density  $n = 23/24$  and exchange coupling  $J/t = 0.8$  for different segment size  $S_l = 2, 4$  and  $6$  as indicated. In each case, the usual  $t$ - $J$  model i.e., hopping modulation  $\delta t = 0$  gives zero spin gap. As we introduce finite  $\delta t$ , the system develops finite spin gap and vanishes again at higher  $\delta t$ . Similarly corresponding binding energy:  $\Delta_b = E(N \pm 2, S_z^T = 0) + E(N, S_z^T = 0) - 2E(N \pm 1, S_z^T = \pm 1/2)$  extrapolations are shown in Fig. 2. The spin gap and binding energies are found to be almost equal.

### LUTTINGER PARAMETER

We find the transition from metallic to SC phase by calculating the Luttinger parameter  $K_\rho < 1$  for metallic and  $K_\rho > 1$  for superconducting phase. In thermodynamic limit Luttinger parameter is calculated from the slope of the structure factor for the density-density correlation at wave vector  $q \rightarrow 0$  limit[3, 4].

$$K_\rho = \pi \lim_{q \rightarrow 0^+} \frac{\widetilde{W}(q)}{q} \quad (2)$$

where for finite systems in numerical simulations  $q = 2\pi/L$ ,  $L$  being the system size and the Fourier transform of correlation,

$$\widetilde{W}(q) = \frac{1}{L} \sum_{l=1}^L (\langle n_i n_{i+l} \rangle - \langle n_i \rangle \langle n_{i+l} \rangle) e^{-iq l}$$

The accuracy of  $K_\rho$  suffers in this approach due to the difficulties in accurate calculation of density-density correlations, specially at large distances and subsequently the Fourier transform at small  $q$ . So we calculate structure factor directly in momentum space[5] and extract  $K_\rho$  in thermodynamic limit by finite size scaling.

For this we define an operator in momentum space:

$$\widetilde{N}(q) = \frac{1}{L} \langle \Psi_0 | \widetilde{n}(q) \widetilde{n}(-q) | \Psi_0 \rangle \quad (3)$$

where  $\widetilde{n}(q) = \sum_{l,\sigma} c_{l\sigma}^\dagger c_{l\sigma} e^{-iq(l-r_c)}$ ;  $r_c = (L+1)/2$  being the middle position of the chain. Note that  $\widetilde{N}(q)$  and  $\widetilde{W}(q)$  are different, but becomes identical only in thermodynamic limit. So finally we get  $K_\rho$  by targeting not only the ground state  $\Psi_0$  but also the state  $\widetilde{n}(q)|\Psi_0\rangle$  as:

$$K_\rho = \lim_{L \rightarrow \infty} \frac{L}{2} \widetilde{N}(2\pi/L) \quad (4)$$

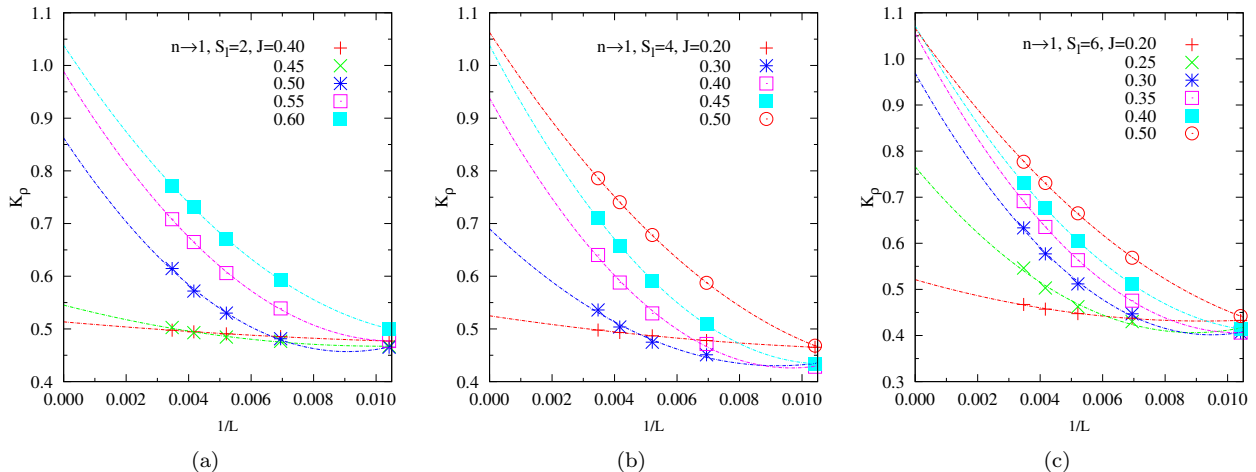


FIG. 3: (Color online) The Luttinger parameter extrapolation to thermodynamic limit for a system with two holes i.e.,  $n \rightarrow 1$  limit at hopping modulation  $\delta t = 0.2$ . These plots are for different exchange coupling  $J$  and segment length  $S_l$  as indicated.

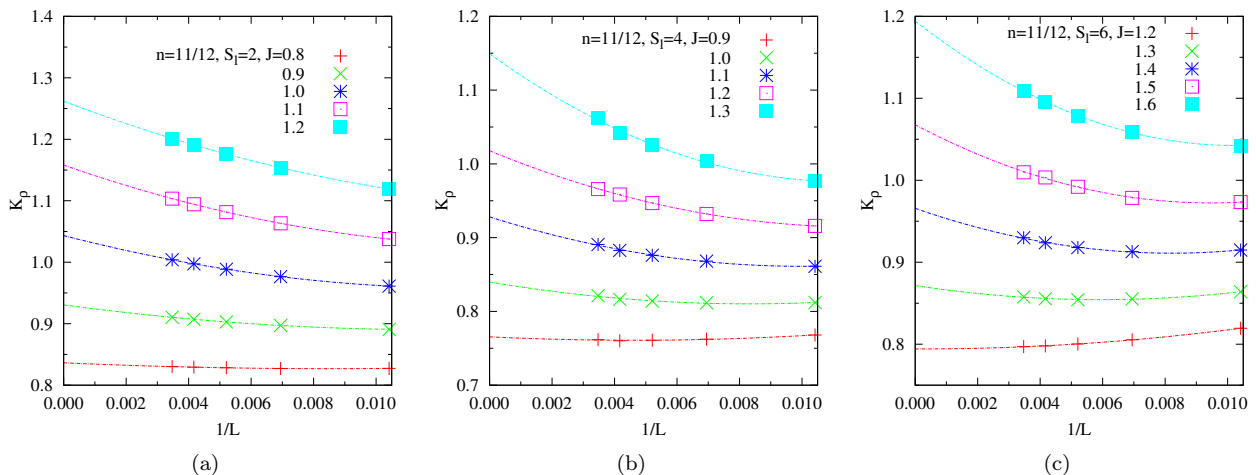


FIG. 4: (Color online) The Luttinger parameter extrapolation to thermodynamic limit for finite density  $n = 11/12$ . These plots are for different exchange coupling  $J$  and segment length  $S_l$  as indicated.

Fig. 3 shows the finite size extrapolation to thermodynamic limit for a system with two holes i.e.,  $n \rightarrow 1$  limit at hopping modulation  $\delta t = 0.2$ . We see for each segment length  $S_l$  the Luttinger parameter  $K_\rho$  in thermodynamic limit goes above  $K_\rho = 1$  value where the metallic to superconducting transition happens. The critical value of exchange coupling  $J^c$  at this transition can be as small as  $\sim 0.35$  as seen in  $S_l = 6$  system. The similar extrapolation of  $K_\rho$  at finite density  $n = 11/12$  and for different  $S_l$  system are shown in Fig. 4. In this way we have calculated  $K_\rho$  in the thermodynamic limit for different  $n$  and  $S_l$  to obtain the  $n - J$  phase diagrams shown in the main text.

### INSULATING LINE PHASES

Due to the hopping modulation, the electrons tend to form some super structure in each segment causing insulating behavior at some commensurate fillings for different  $S_l$  systems as shown in  $n - J$  phase diagrams in main text. Here we show charge gap  $\Delta_c$  extrapolation to thermodynamic limit to show the melting of insulating phase to metallic state as we increase  $J$ .

As we discussed in detail in the main text that for  $S_l = 2$  system at  $n = 1/2$ , the competition between  $t$ - and  $J$ -dimerization causes the melting to metallic states as we increase  $J$ . Here we discuss insulating lines for  $S_l = 4$



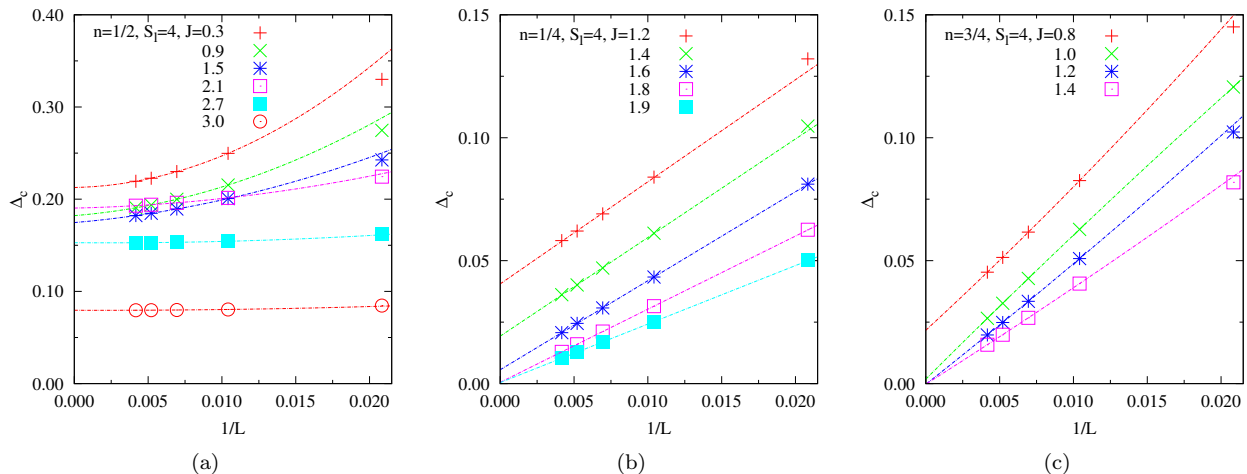


FIG. 5: (Color online) Typical charge gap extrapolation to thermodynamic limit for commensurate densities for  $S_l = 4$  system as we increase  $J$ .

(Fig. 3(b) in main text) system in detail with the help of charge gap extrapolation. At  $n = 1/2$  we notice that the  $S_l = 4$  system is insulating for all values of  $J$  up to phase separation. This is because two  $t$ -dimers are formed in each segment for small  $J$  and accommodate two electrons in bonding states of each  $t$ -dimer at this commensurate filling giving a Mott insulator. When we increase  $J$ , these two electrons already in bonding states lower the energy by pairing themselves. So this insulating phase cannot melt away with increasing  $J$  like the  $S_l = 2$  system at  $n = 1/2$  (discussed in main text). The insulating line phases are captured by calculating the charge gap defined as:

$$\Delta_c = \frac{E(N+2) + E(N-2) - 2E(N)}{2} \quad (5)$$

Fig. 5(a) shows the extrapolation of charge gap to thermodynamic limit at  $n = 1/2$  for  $S_l = 4$  system. The charge gap remains finite for all values of  $J$  upto phase separation. However the melting of insulating states is possible at  $n = 1/4$  and  $3/4$ . At small  $J$ , one electron per segment (i.e.,  $n = 1/4$ ) occupies the lowest energy state formed by superposition of two bonding states already formed by  $t$ -dimerization. Also for  $n = 3/4$ , one electron sits on a  $t$ -dimer formed on middle two sites and other two electrons occupy the ends sites of each segment. As we increase  $J$ , the tendency of  $J$ -dimerization destroys both the insulating states at  $n = 1/4$  and  $3/4$ . Fig. 5(b) and (c) show that the charge gap vanishes as we increase  $J$ . It is intuitive that odd number of electrons in a segment is not suitable for effective pairings and lead to melting of insulating states as we increase  $J$ . Even number of electrons on the other hand can form an effective pairing which prevents the melting of insulating states as shown for  $n = 1/2$  in  $S_l = 4$  system.

Fig. 3(c) of main text depicts the insulating lines at different fillings for  $S_l = 6$  system. At  $n = 1/2$ , three electrons occupy bonding states in three  $t$ -dimers formed in each segment for small  $J$  leading to a Mott insulator. Again like  $S_l = 4$  system at  $n = 1/4$  and  $3/4$ , the odd number of electrons in each segment can't make effective pair. So with increasing  $J$  we have melting of insulating state at  $n = 1/2$  due to the competition of  $t$ - and  $J$ -dimerization. The similar argument holds for  $n = 1/6$  and  $5/6$ . But with even number of electrons at  $n = 2/6$  and  $4/6$  form effective pairs as discussed in  $S_l = 4$  system. So the system continues to be insulating upto phase separation.

Finally in the phase separation the interaction between electrons becomes very large and the electrons forms antiferromagnetic domains such that the system separates into particle- and hole-rich region. We determine the phase separation boundary by calculating inverse compressibility defined as:

$$\chi^{-1} = \frac{N^2}{4}(E(N+2) + E(N-2) - 2E(N)) \quad (6)$$

After extrapolating energy to thermodynamic limit, we calculate  $\chi^{-1}$  as a function of  $J$  and obtain the phase separation boundary. Fig. 6 shows typical plot of  $\chi^{-1}$  as function of  $J$  at  $n = 1/4, 1/2$  and  $3/4$  for  $S_l = 4$  system. We consider the crossing of  $\chi^{-1}$  at zero line as onset of phase separation.

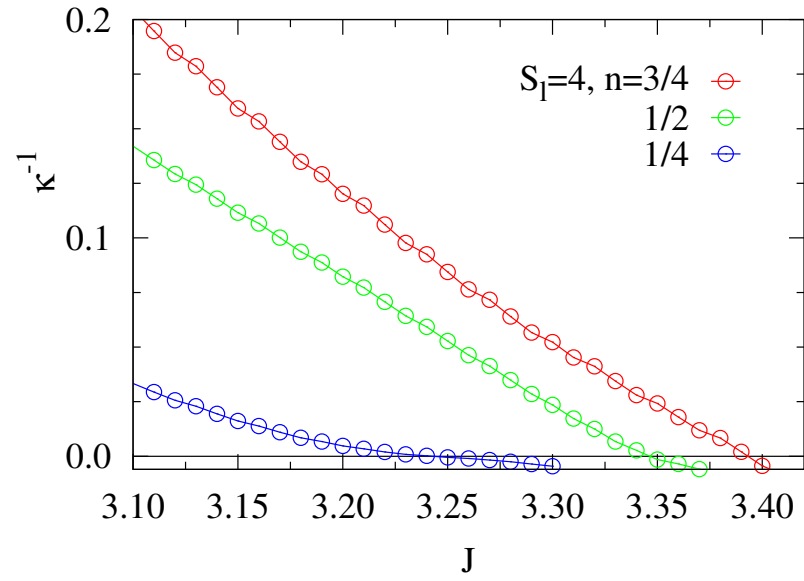


FIG. 6: (Color online) Inverse compressibility  $\chi^{-1}$  as a function of  $J$  at different electron density for  $S_l = 4$  system

- 
- [1] S. R. White, Phys. Rev. Lett. **69**, 2863 (1992)
  - [2] U. Schollwock, Rev. Mod. Phys. **77**, 259 (2005)
  - [3] T. Giamarchi, Quantum Physics in One Dimension (Clarendon, Oxford, UK, 2004)
  - [4] R. T. Clay et al., Phys. Rev. B **59**, 4665 (1999)
  - [5] S. Ejima et al., Eurphys. Lett. **70**, 492 (2005)